Icarus 251 (2015) 5–11

Contents lists available at ScienceDirect

Icarus

journal homepage: www.elsevier.com/locate/icarus

Variations in peak electron densities in the ionosphere of Mars over a full solar cycle

Paul Withers [a,*], D.D. Morgan [b], D.A. Gurnett [b]

[a] Astronomy Department, Boston University, 725 Commonwealth Avenue, Boston, MA 02215, USA
[b] Department of Physics, University of Iowa, 203 Van Allen Hall, Iowa City, IA 52242, USA

ARTICLE INFO

Article history:
Received 19 February 2014
Revised 24 June 2014
Accepted 11 August 2014
Available online 23 August 2014

Keywords:
Mars
Ionosphere
Solar radiation

ABSTRACT

Peak electron densities in the ionosphere of Mars are strongly influenced by the intensity of ionizing solar flux and hence by the solar cycle. Datasets used in previous studies of this relationship have incompletely sampled the range of solar irradiances encountered over a full solar cycle. Here, thousands of Mars Global Surveyor radio occultation measurements and hundreds of thousands of Mars Express topside radar sounder measurements from 1998 to 2013 are used to test whether the conclusions of previous workers withstand a substantial increase in the number of datapoints and near-continuous sampling across a range of ionizing solar irradiances. Data from narrow ranges in solar zenith angle (70°–80°) and latitude (60°N–80°N) are used in order to isolate, to the extent possible, the influence of irradiance. Ionospheric peak electron density increases smoothly with increasing F10.7, but this increase saturates at F10.7 values above 130 units. However, in contrast to some previous work, there is no change in behavior at an F10.7 value of 100 units. Saturation at high values of F10.7 also occurs in Earth's ionosphere and the underlying cause is that the appropriateness of F10.7 as a proxy for ionizing solar irradiance diminishes at high solar activity. Similar overall trends are seen when the Lyman alpha emission or the Mg II core-to-wing index are used to replace F10.7 as a proxy for ionizing solar irradiance. Even when solar zenith angle and latitude are restricted, a time series of electron density residuals shows noteworthy trends. These trends might indicate a dependence of peak density on season, but they are not caused by changes in the Mars–Sun distance.

1. Introduction

Orbital spacecraft have continuously operated at Mars since the arrival of Mars Global Surveyor (MGS) in 1997. These missions (Mars Global Surveyor, Mars Odyssey, Mars Express (MEX), Mars Reconnaissance Orbiter) have provided long-term monitoring of a host of features related to the geology, climate, and space environment of Mars. Ionospheric observations have been provided by radio occultation observations by MGS and MEX (Hinson et al., 1999; Pätzold et al., 2005) and by topside radio sounder observations by the MARSIS instrument on MEX (Gurnett et al., 2005, 2008). Both types of observations determine the peak electron density in the dayside ionosphere, which is the single most useful diagnostic of the state of the ionosphere and the focus of this work.

Dayside electron densities in the ionosphere are affected by the solar cycle, with densities increasing as ionizing solar irradiance increases. Many workers have investigated how peak electron density changes with various representations of the ionizing solar irradiance (Hantsch and Bauer, 1990; Breus et al., 2004; Withers and Mendillo, 2005; Zou et al., 2006; Morgan et al., 2008; Fox, 2004; Fox and Yeager, 2006, 2009; Němec et al., 2011; Girazian and Withers, 2013). However, due to limited amounts of data, none have yet looked at variations in peak electron density with time over a full solar cycle.

Here we investigate how peak electron densities observed by MGS radio occultations and MEX topside radar sounding observations from MARSIS vary with time from 1998 to 2013. This period encompasses a strong solar maximum in 2000 and a remarkably prolonged and deep solar minimum centered on 2008. Our primary objective is to test whether the conclusions of previous workers withstand a substantial increase in the number of datapoints and near-continuous sampling across a range of ionizing solar irradiances. Secondary objectives are to investigate whether changes in season and local solar time have significant effects on peak electron density.

Fig. 1 shows solar conditions, the Mars–Sun distance, martian season, observed solar zenith angle, and observed latitude during this period. Times are described by "Day of year 1998" such that

* Corresponding author.

http://dx.doi.org/10.1016/j.icarus.2014.08.008
0019-1035/

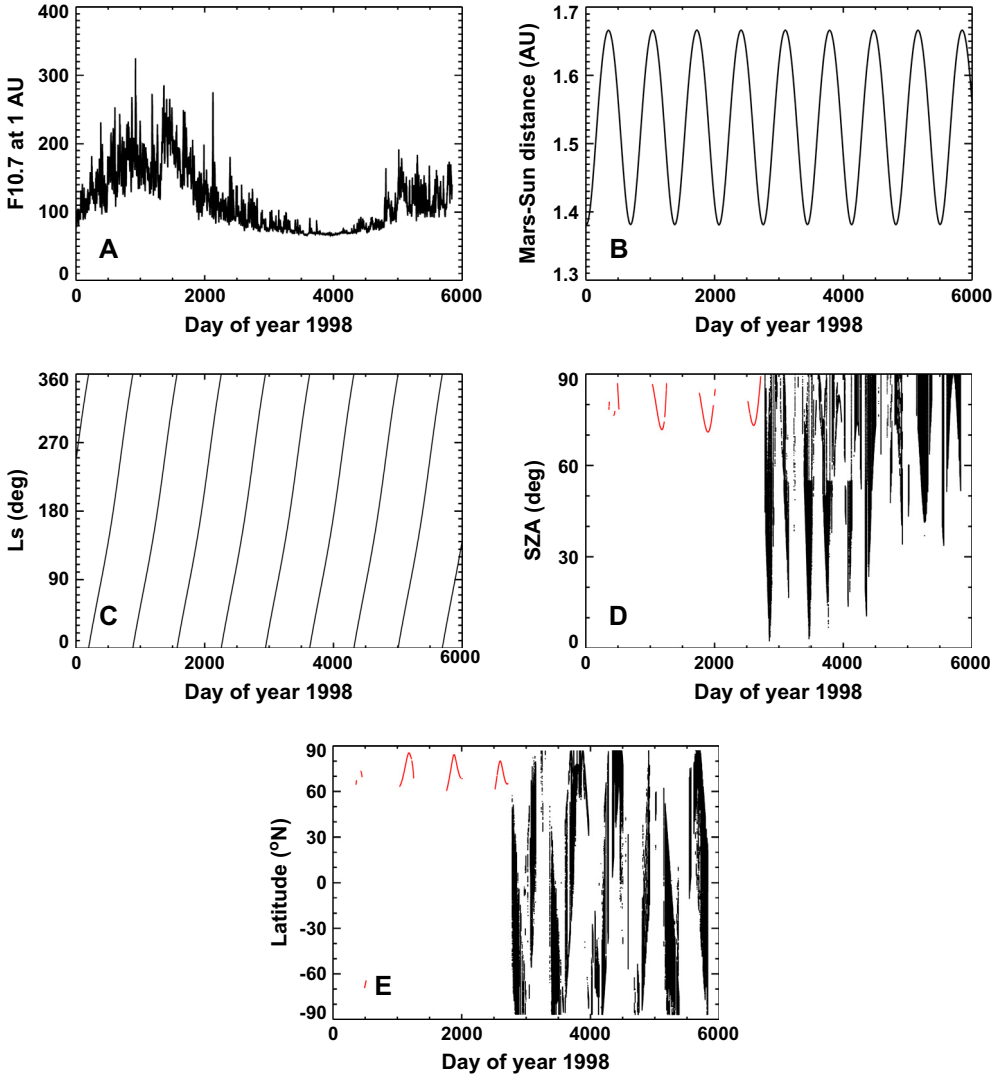

Fig. 1. A. Solar irradiance at 1 AU. These F10.7 values were obtained from the National Geophysical Data Center, ftp://ftp.ngdc.noaa.gov/STP/space-weather/solar-data/solar-features/solar-radio/noontime-flux/penticton/penticton_adjusted/listings/listing_drao_noontime-flux-adjusted_daily.txt. B. Mars–Sun distance. C. Ls, a measure of martian season. D. Solar zenith angle of ionospheric observations by MGS radio occultations (red) and MARSIS (black). E. Latitude of ionospheric observations by MGS radio occultations (red) and MARSIS (black). (For interpretation of the references to color in this figure legend, the reader is referred to the web version of this article.)

1 January 1998 equals 1 and 31 December 2013 equals 5843. Fig. 1 uses the value of F10.7 at 1 AU to illustrate variations in the ionizing solar irradiance over time. This solar irradiance proxy is admittedly imperfect, but has the advantage of being widely used in prior work (e.g., Hantsch and Bauer, 1990; Morgan et al., 2008) and available over many decades (Girazian and Withers, 2013). Other proxies for the ionizing solar irradiance are discussed later in this work (Section 3).

Section 2 introduces the two datasets, MGS radio occultations and MARSIS topside radar soundings, and describes the preparation of the data. Section 3 describes trends in electron densities over the solar cycle (Section 3.1) and interprets the residual differences between observations and a fit to the observations (Section 3.2). Section 4 presents our conclusions.

2. Observations and data preparation

MGS radio occultations determined 5600 electron density profiles at solar zenith angles less than 90°. The dates, latitudes, and solar zenith angles (SZAs) sampled by this dataset are listed in Table 1 of Withers et al. (2008) (Fig. 1). These data were acquired from the Planetary Data System (Hinson, 2007). Previous workers have used these observations to track tides in the neutral thermosphere (Bougher et al., 2001, 2004), to characterize the ionospheric effects of crustal magnetic fields (Withers et al., 2005), to study layers of meteoric plasma (Withers et al., 2008), and to investigate the ionospheric effects of the changing solar irradiance (Withers and Mendillo, 2005; Mendillo et al., 2006; Girazian and Withers, 2013). The 5600 peak electron densities are shown in the top panel of Fig. 2.

MARSIS topside radar sounding produced over 140,000 ionograms at solar zenith angles less than 90° between 14 August 2005 and 12 December 2013. Previous workers have used these observations to discover ionospheric bulges over regions of strong crustal magnetic fields (Duru et al., 2006), to characterize a sporadic layer in the topside ionosphere (Kopf et al., 2008), to detect the ionopause (Duru et al., 2009), to monitor the radio wave attenuation caused by solar energetic particle events (Morgan et al., 2006, 2010), to explore the nightside ionosphere (Němec et al., 2010, 2011; Duru et al., 2011), to develop an empirical model of ionospheric densities (Němec et al., 2011), to quantify the ionospheric effects of seasonal and solar variations (Morgan et al.,

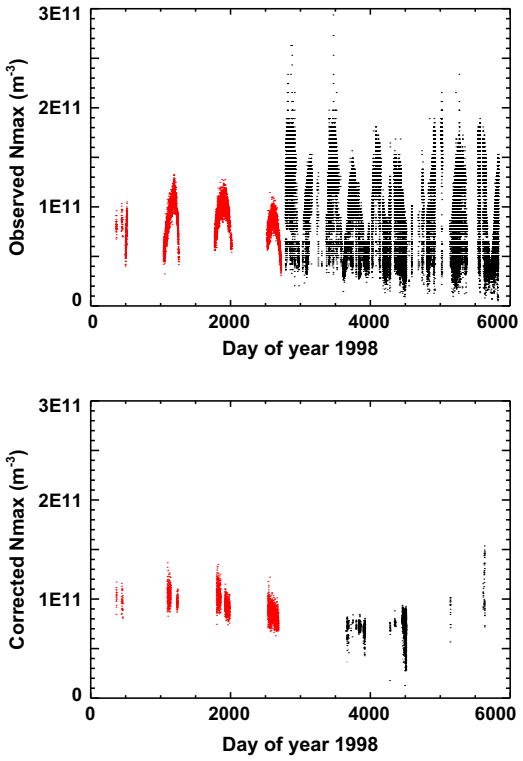

Fig. 2. Top. Peak electron densities observed by MGS radio occultations (red) and MARSIS (black). Bottom. Selected corrected peak electron densities from MGS radio occultations (red) and MARSIS (black). Only data with 70° < SZA < 80° and latitudes between 60°N and 80°N are selected. (For interpretation of the references to color in this figure legend, the reader is referred to the web version of this article.)

2008) and to extend measurements of peak electron density to the subsolar point (Gurnett et al., 2005, 2008). The over 140,000 peak electron densities are shown in the top panel of Fig. 2. The instrumental discretization, which is not uniform in electron density (Gurnett et al., 2008; Morgan et al., 2013), is particularly visible at large electron densities.

Since these two instruments operated at different periods, they never observed the same location on Mars at the same time. That is an obstacle to demonstrating that results from the two instruments are directly comparable. However, Morgan et al. (2008) validated MARSIS results against MGS and MEX radio occultation data, and concluded that the "sounding [MARSIS] and radio occultation methods are in approximate agreement in the near-peak region below 200 km altitude for solar zenith angles between 75° and 80°." The main disagreement noted by Morgan et al. (2008) concerned the altitude scales, which does not affect this work at all. Furthermore, no systematic differences between topside sounder data and radio occultation data have been suggested from studies at Earth.

The observed electron densities must be corrected for an obvious strong dependence on SZA. In order to do so, we adjust each observed peak density to SZA = 75° assuming a Chapman-like dependence on SZA (Withers, 2009). To minimize the effects of potential errors in this correction, only data taken at 70° < SZA < 80° are used. We also adjust for variations in the Mars–Sun distance by assuming that peak density is inversely proportional to the Mars–Sun distance (Mendillo et al., 2003). Peak electron density may also depend on latitude due to meridional variations in atmospheric properties. This possible issue is minimized by using only data taken at latitudes between 60°N and 80°N. Selection of northern polar latitudes in this work removes all sensitivity to crustal magnetic fields, which Nielsen et al. (2007) found to influence peak densities. We identify the resultant electron densities as corrected peak densities and show them in the bottom panel of Fig. 2. After this culling, 2910 MGS and 2778 MARSIS peak densities are retained.

Substantial scatter is present in these data. We reduce this scatter for each dataset in turn by finding the average of all corrected peak densities from a given day. This yields 360 MGS radio occultation and 112 MARSIS daily average corrected peak densities.

3. Analysis

3.1. Solar cycle effects

The daily average corrected peak densities are shown in Fig. 3. One MARSIS daily average corrected peak density (DOY 1998 = 5629, 30 May 2013) is an outlier with a value of more than 1.2×10^{11} m^{-3}. This is not skewed by a single rogue datum since the average is based upon 8 measurements that range from 1.2×10^{11} m^{-3} to 1.4×10^{11} m^{-3}. Since the data themselves do not appear to be flawed or suspect, these high values merit attention. One possible explanation could be that a solar flare occurred on that date, when Earth and Mars were on opposite sides of the Sun. Solar flares have been observed to increase peak densities for short periods (Gurnett et al., 2005; Mendillo et al., 2006; Nielsen et al., 2006). Although no large flare was observed at Earth on 30 May 2013, four X-class solar flares were detected in that month (Watanabe et al., 2012). It is therefore possible that a solar flare that was not visible from Earth is responsible for these elevated densities.

Densities increase with time to a maximum at days 1000–2000, decrease to a minimum at days 3500–4000, and increase thereafter. These time variations track those of the solar cycle, which is most evident when illustrated with the 81-day (3 solar rotation periods) running average of F10.7 (Richards et al., 1994), which is shown in Fig. 3. We use this long-term average of solar irradiance here since the daily measurements of F10.7 made at Earth are not precisely applicable at Mars. F10.7 is measured at Earth, and Mars and Earth often face different hemispheres of the Sun. Using the 81-day average compensates somewhat for this problem.

Fig. 3 shows that ionospheric densities increase as the ionizing solar irradiance increases. Note that there is no obvious systematic difference between the two types of data, MGS and MARSIS, used in this work. Compared to previous studies of this topic, Fig. 3 fills in many gaps present in Fig. 4 of Hantsch and Bauer (1990) and extends the range of Fig. 8 of Morgan et al. (2008). There is no suggestion that the rate of change of density with respect to irradiance changes abruptly at F10.7 = 100 units, which was indicated by the results of Hantsch and Bauer (1990). The rate of change of density with respect to irradiance is markedly reduced at high solar irradiances and peak electron densities scarcely increase as solar irradiances increase from 130 units to 170 units. This "saturation" has a well-known analog in the terrestrial ionosphere (Titheridge, 1997; Liu et al., 2009) and was previously noted at Mars by Mendillo et al. (2013).

However, this does not mean that ionospheric peak densities reach a ceiling as the ionizing solar irradiance increases without limit. Instead, this saturation occurs because F10.7 becomes less useful as a proxy for ionizing solar irradiance at very high solar irradiances (Chamberlin et al., 2007). At very high solar irradiances, small increases in actual ionizing irradiance are associated with large increases in F10.7. This was demonstrated at Mars by Girazian and Withers (2013), who investigated the dependence of MGS radio occultation peak electron densities on the ionizing solar irradiance by using direct TIMED-SEE measurements of the solar spectrum, rather than an indirect proxy. Girazian and

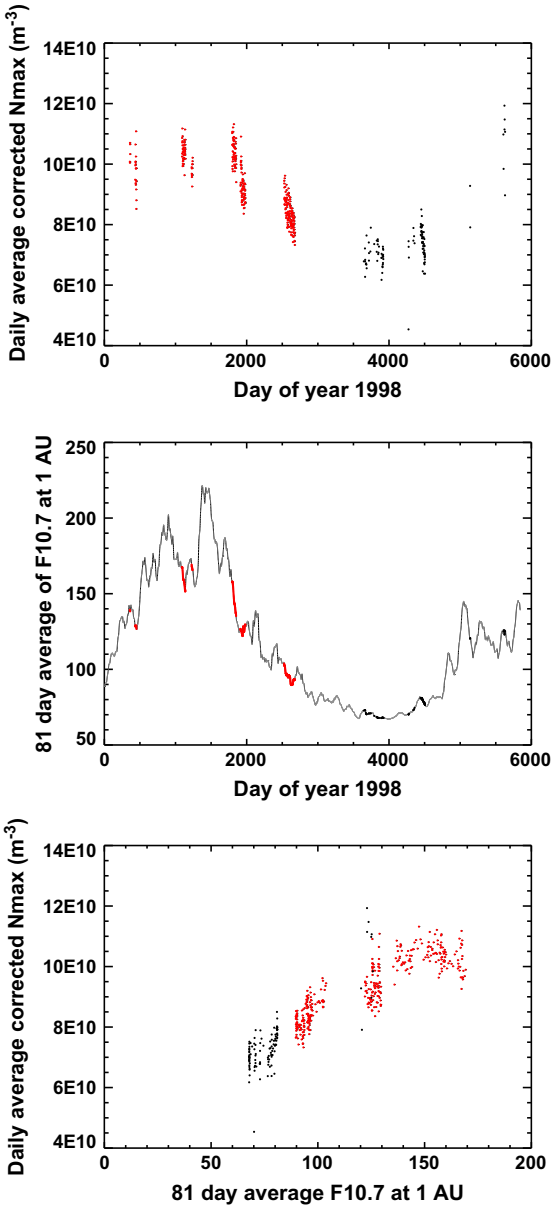

Fig. 3. Top. Selected daily-averaged corrected peak electron densities from MGS radio occultations (red) and MARSIS (black). Only data with 70° < SZA < 80° and latitudes between 60°N and 80°N are selected. Middle. 81 day average of the solar irradiance at 1 AU (gray line). Values on the days for which selected ionospheric data are available are shown by colored disks: MGS radio occultations (red) and MARSIS (black). Bottom. Selected daily-averaged corrected peak electron densities as a function of the 81 day average of the solar irradiance at 1 AU. Colors indicate dataset: MGS radio occultations (red) and MARSIS (black). (For interpretation of the references to color in this figure legend, the reader is referred to the web version of this article.)

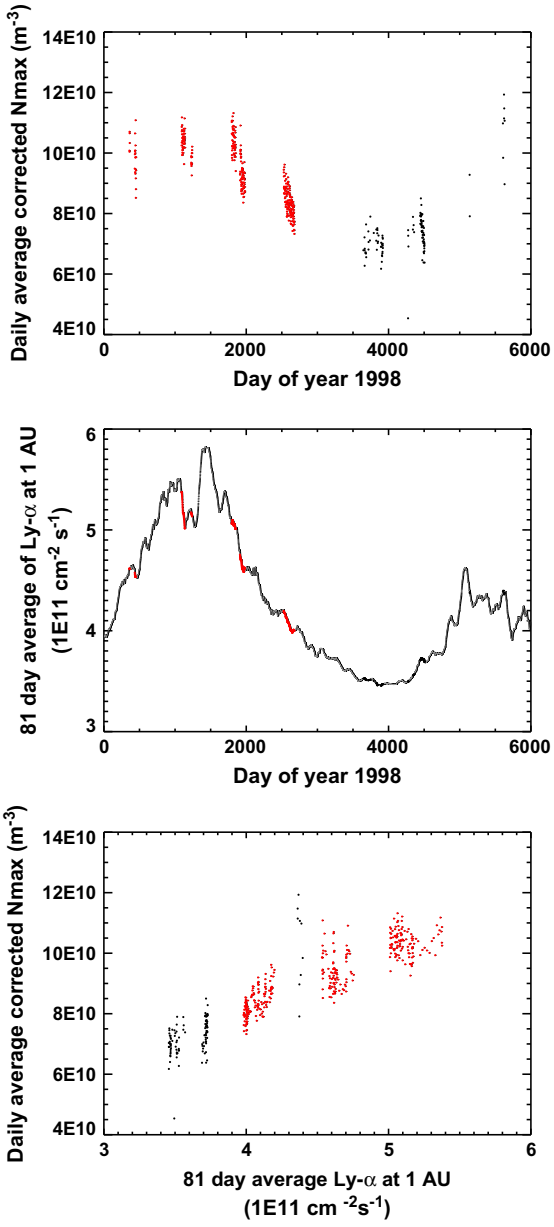

Fig. 4. As Fig. 3, but using Lyman alpha emission as a proxy for solar irradiance. These Lyman alpha data were obtained from the LASP Interactive Solar IRradiance Data Center (LISIRD) at the University of Colorado, http://lasp.colorado.edu/lisird/.

Withers (2013) used the TIMED-SEE data to determine the total number of ionization events attributable to sunlight per unit area per unit time, which is equivalent to the "total ionizing flux" in introductory descriptions of ionospheric processes, and found that the dependence of peak electron density on this quantity did not saturate at large irradiances.

The limitations of F10.7 as a proxy for the ionizing solar irradiance are well-known. Accordingly, Figs. 4 and 5 show versions of Fig. 3 in which solar irradiance is represented by solar Lyman-alpha emission and the Mg II core-to-wing index, respectively (Chamberlin et al., 2007). Both figures show that peak electron density increases steadily as the proxy for ionizing solar irradiance increases.

3.2. Residuals

The MGS densities in the top panel of Fig. 3 can be classified into four groups about 700 days apart, each containing two sub-groups. These groupings are caused by the nature of the MGS orbit. It is striking that, for every group, densities in the second sub-group are always smaller than densities in the first sub-group. If the 347 MGS daily average corrected peak densities are fit by $N = N_0 F^k$, where N_0 is a reference density, F is the 81 day average of the Mg II core-to-wing index, and k is an exponent, then the best fit parameters are $N_0 = 8.3 \times 10^{14}$ m^{-3} and $k = 7.0$. Here we have elected to use the Mg II core-to-wing index as a proxy for the ionizing solar irradiance, since it yields a smaller root-mean-square residual (1.05×10^8 m^{-3}) than the F10.7 index (1.19×10^8 m^{-3})

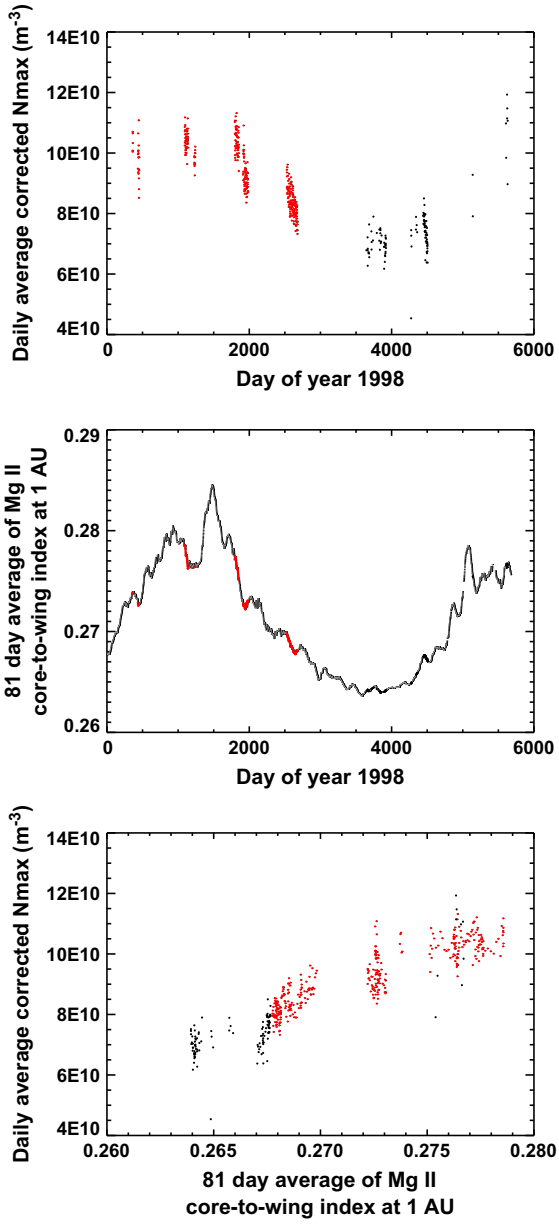

Fig. 5. As Fig. 3, but using the Mg II core-to-wing index as a proxy for solar irradiance. These Mg II data were obtained from the LASP Interactive Solar IRradiance Data Center (LISIRD) at the University of Colorado, http://lasp.colorado.edu/lisird/.

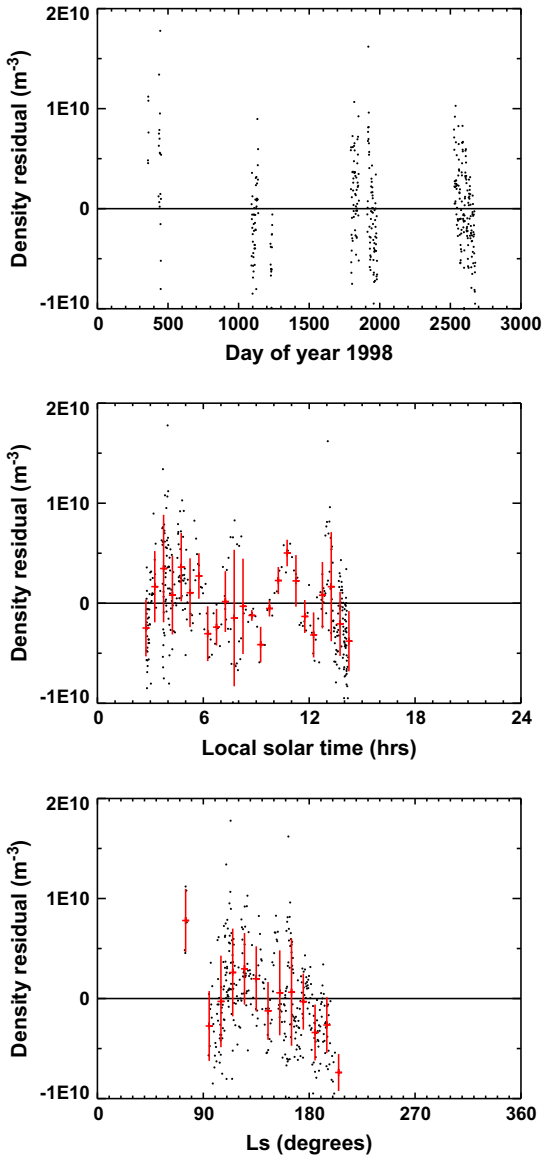

Fig. 6. Top. Residuals from a fit of the dependence of selected MGS daily-averaged corrected peak electron densities on the Mg II core-to-wing index are shown as a function of time. Only data with 70° < SZA < 80° and latitudes between 60°N and 80°N are selected. Middle. The same residuals (black points) as a function of local solar time. The red crosses show the average residual for intervals 0.5 h wide and the vertical red lines show the corresponding standard deviations. Bottom. The same residuals as a function of season. The red crosses show the average residual for intervals 10 degrees of Ls wide and the vertical red lines show the corresponding standard deviations. (For interpretation of the references to color in this figure legend, the reader is referred to the web version of this article.)

or the Lyman alpha emission (1.13×10^8 m^{-3}). The top panel of Fig. 6 shows the residuals between the MGS densities and this fit as a function of time.

It is clear that the MGS daily average corrected peak densities are influenced by at least one other factor in addition to solar irradiance. The most obvious potential factors that might give rise to this effect are local solar time, season, and Mars–Sun distance. Although we have corrected for the Mars–Sun distance in preparing these data products, that correction was based on the assumption that peak densities are inversely proportional to Mars–Sun distance, consistent with peak densities being proportional to the square root of the ionizing solar irradiance (Mendillo et al., 2003). It is possible that this assumption is imperfect.

The middle and bottom panels of Fig. 6 shows the residuals between the MGS densities and this fit as functions of local solar time and season, respectively. This figure shows that season could be a possible cause of the striking trends in the residuals. One way in which season could affect peak density is via the neutral scale height. In idealized Chapman theory, the square of the peak density is inversely proportional to the neutral scale height (Withers, 2009). In this scenario, the possible seasonal trend in the residuals implies a seasonal minimum in temperature around Ls = 120°. There are few measurements of thermospheric temperatures in the northern polar regions, but a striking temperature maximum does occur at the opposite season (Bougher et al., 2006).

Fig. 6 does not show a clear trend in the residuals with local solar time. If Mars–Sun distance were the sole cause of the residuals, then they would be symmetric about aphelion (Ls = 71°). Although the residuals do not extend to the pre-aphelion season,

there is little indication that the residuals are independent of Ls in the near-aphelion season, which disfavors the Mars–Sun distance as a possible cause of the trends in the residuals.

In a flawless study of the ionospheric response to changing solar irradiance, a single instrument would observe ionospheric densities at fixed solar zenith angle, latitude, local solar time, and season while the solar irradiance varies substantially. Such an experiment is obviously not possible. We have attempted to approach this ideal by severely restricting the solar zenith angles and latitudes at which data are used, but the residuals show that other influences remain present. It is therefore worthwhile to consider whether these restrictions have actually improved the results of this work or not. Fig. 7 ignores the solar zenith angle and latitude restrictions imposed in the rest of this work and shows 683 MGS and 1081 MARSIS daily average corrected peak densities from across the solar cycle. The fundamental trends are still visible, but the scatter in the peak densities at a given solar irradiance is appreciably greater than before. The imposition of narrow ranges in solar zenith angle and latitude has therefore improved the clarity of the results.

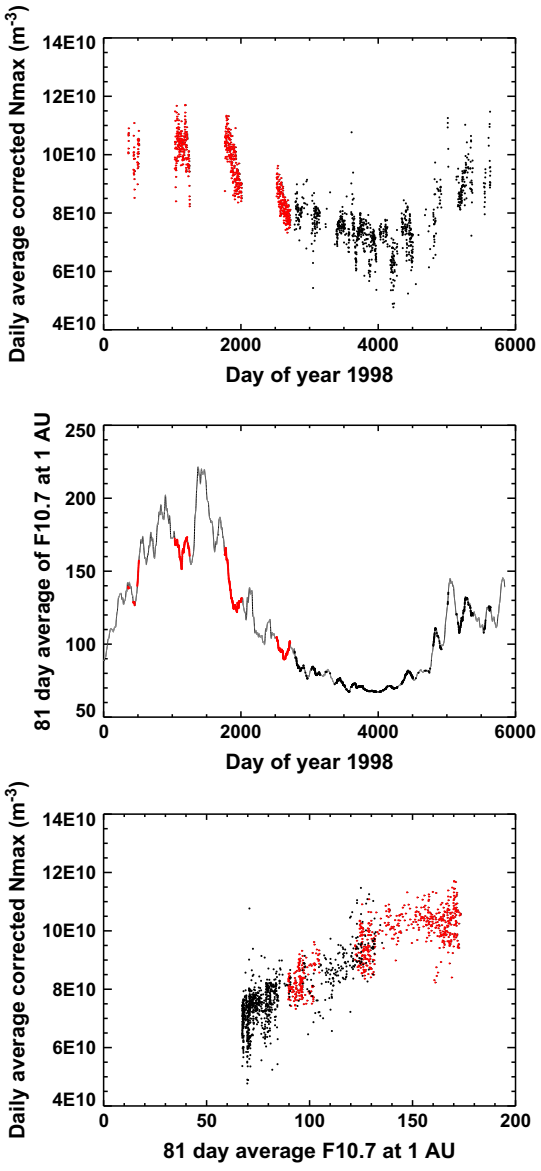

Fig. 7. As Fig. 3, but without the restrictions on solar zenith angle and latitude.

4. Conclusions

This study has used thousands of MGS radio occultation measurements and hundreds of thousands of MARSIS topside soundings to comprehensively sample the peak electron density in the ionosphere of Mars over 15 years, longer than a full solar cycle, and spanning 81-day average F10.7 values at 1 AU from 70 to 170 units. There is no suggestion that the rate of change of density with respect to irradiance changes abruptly at an F10.7 value of 100 units, which was indicated by the results of Hantsch and Bauer (1990). Instead, ionospheric peak electron density increases smoothly with increasing F10.7 up to an F10.7 value of 130 units, although there is substantial scatter in the data points. As F10.7 increases above 130 units, the increase in peak density saturates. Analogous saturation also occurs in Earth's ionosphere and the underlying cause is that the appropriateness of F10.7 as a proxy for ionizing solar irradiance diminishes at high solar activity. Similar trends are seen when the Lyman alpha emission or the Mg II core-to-wing index are used to replace F10.7 as a proxy for ionizing solar irradiance: peak density increases as the solar irradiance proxy increases and peak density saturates at high values of the solar irradiance proxy.

Even after solar zenith angle and latitude are restricted, a time series of electron density residuals shows noteworthy trends. These trends might indicate a dependence of peak density on season via seasonal variations in thermospheric temperature and scale height. These trends are not caused by changes in the Mars–Sun distance.

Although solar irradiance plays a major role in determining the peak density in the ionosphere of Mars, as is evident from the strong trends presented in this work, other factors that are as yet poorly-determined also play roles. Neutral composition, neutral temperature, and magnetospheric conditions might be among these other factors. It may be possible to better understand those other factors in the near future using the comprehensive observations anticipated from the MAVEN mission.

Acknowledgments

We gratefully acknowledge three anonymous reviewers and the providers of the publicly available ionospheric and solar data used in this work. This work was supported, in part, by NASA award NNX12AJ39G (PW). DM and DG acknowledge support from JPL contract 1224107 to the University of Iowa.

References

Bougher, S.W., Engel, S., Hinson, D.P., Forbes, J.M., 2001. Mars Global Surveyor Radio Science electron density profiles: Neutral atmosphere implications. Geophys. Res. Lett. 28, 3091–3094.

Bougher, S.W., Engel, S., Hinson, D.P., Murphy, J.R., 2004. MGS Radio Science electron density profiles: Interannual variability and implications for the martian neutral atmosphere. J. Geophys. Res. 109, E03010. http://dx.doi.org/10.1029/2003JE002154.

Bougher, S.W., Bell, J.M., Murphy, J.R., Lopez-Valverde, M.A., Withers, P.G., 2006. Polar warming in the Mars thermosphere: Seasonal variations owing to changing insolation and dust distributions. Geophys. Res. Lett. 33, L02203. http://dx.doi.org/10.1029/2005GL024059.

Breus, T.K., Krymskii, A.M., Crider, D.H., Ness, N.F., Hinson, D., Barashyan, K.K., 2004. Effect of the solar radiation in the topside atmosphere/ionosphere of Mars: Mars Global Surveyor observations. J. Geophys. Res. 109, A09310. http://dx.doi.org/10.1029/2004JA010431.

Chamberlin, P.C., Woods, T.N., Eparvier, F.G., 2007. Flare Irradiance Spectral Model (FISM): Daily component algorithms and results. Space Weather 5, S07005. http://dx.doi.org/10.1029/2007SW000316.

Duru, F. et al., 2006. Magnetically controlled structures in the ionosphere of Mars. J. Geophys. Res. 111, A12204. http://dx.doi.org/10.1029/2006JA011975.

Duru, F., Gurnett, D.A., Frahm, R.A., Winningham, J.D., Morgan, D.D., Howes, G.G., 2009. Steep, transient density gradients in the martian ionosphere similar to the ionopause at Venus. J. Geophys. Res. 114, A12310. http://dx.doi.org/10.1029/2009JA014711.

Duru, F., Gurnett, D.A., Morgan, D.D., Winningham, J.D., Frahm, R.A., Nagy, A.F., 2011. Nightside ionosphere of Mars studied with local electron densities: A general overview and electron density depressions. J. Geophys. Res. 116, A10316. http://dx.doi.org/10.1029/2011JA016835.

Fox, J.L., 2004. Response of the martian thermosphere/ionosphere to enhanced fluxes of solar soft X rays. J. Geophys. Res. 109, A11310. http://dx.doi.org/10.1029/2004JA010380.

Fox, J.L., Yeager, K.E., 2006. Morphology of the near-terminator martian ionosphere: A comparison of models and data. J. Geophys. Res. 111, A10309. http://dx.doi.org/10.1029/2006JA011697.

Fox, J.L., Yeager, K.E., 2009. MGS electron density profiles: Analysis of the peak magnitudes. Icarus 200, 468–479.

Girazian, Z., Withers, P., 2013. The dependence of peak electron density in the ionosphere of Mars on solar irradiance. Geophys. Res. Lett. 40, 1960–1964.

Gurnett, D.A. et al., 2005. Radar soundings of the ionosphere of Mars. Science 310, 1929–1933.

Gurnett, D.A. et al., 2008. An overview of radar soundings of the martian ionosphere from the Mars Express spacecraft. Adv. Space Res. 41, 1335–1346.

Hantsch, M.H., Bauer, S.J., 1990. Solar control of the Mars ionosphere. Planet. Space Sci. 38, 539–542.

Hinson, D.P., 2007. MGS RST Science Data Products, USA_NASA_JPL_MORS_1102. In: Simpson, R.A. (Ed.), MGS-M-RSS-5-EDS-V1.0. NASA Planetary Data System.

Hinson, D.P., Simpson, R.A., Twicken, J.D., Tyler, G.L., Flasar, F.M., 1999. Initial results from radio occultation measurements with Mars Global Surveyor. J. Geophys. Res. 104, 26997–27012.

Kopf, A.J., Gurnett, D.A., Morgan, D.D., Kirchner, D.L., 2008. Transient layers in the topside ionosphere of Mars. Geophys. Res. Lett. 35, L17102. http://dx.doi.org/10.1029/2008GL034948.

Liu, L., Wan, W., Ning, B., Zhang, M.-L., 2009. Climatology of the mean total electron content derived from GPS global ionospheric maps. J. Geophys. Res. 114, A06308. http://dx.doi.org/10.1029/2009JA014244.

Mendillo, M., Smith, S., Wroten, J., Rishbeth, H., Hinson, D., 2003. Simultaneous ionospheric variability on Earth and Mars. J. Geophys. Res. 108, 1432. http://dx.doi.org/10.1029/2003JA009961.

Mendillo, M., Withers, P., Hinson, D., Rishbeth, H., Reinisch, B., 2006. Effects of solar flares on the ionosphere of Mars. Science 311, 1135–1138.

Mendillo, M., Marusiak, A., Withers, P., Morgan, D., Gurnett, D., 2013. A new semiempirical model of the peak electron density of the martian ionosphere. Geophys. Res. Lett. 40, 5361–5365.

Morgan, D.D. et al., 2006. Solar control of radar wave absorption by the martian ionosphere. Geophys. Res. Lett. 33, L13202. http://dx.doi.org/10.1029/2006GL026637.

Morgan, D.D., Gurnett, D.A., Kirchner, D.L., Fox, J.L., Nielsen, E., Plaut, J.J., 2008. Variation of the martian ionospheric electron density from Mars Express radar soundings. J. Geophys. Res. 113, A09303. http://dx.doi.org/10.1029/2008JA013313.

Morgan, D.D., Gurnett, D.A., Kirchner, D.L., Winningham, J.D., Frahm, R., Brain, D.A., Mitchell, D.L., Luhmann, J.G., Nielsen, E., Espley, J.R., Acuña, M.H., Plaut, J.J., 2010. Radar absorption due to a corotating interaction region encounter with Mars detected by MARSIS. Icarus 206, 95–103.

Morgan, D.D., Witasse, O., Nielsen, E., Gurnett, D.A., Duru, F., Kirchner, D.L., 2013. The processing of electron density profiles from the Mars Express MARSIS topside sounder. Radio Sci. 48, 197–207.

Němec, F., Morgan, D.D., Gurnett, D.A., Duru, F., 2010. Nightside ionosphere of Mars: Radar soundings by the Mars Express spacecraft. J. Geophys. Res. 115, E12009. http://dx.doi.org/10.1029/2010JE003663.

Němec, F., Morgan, D.D., Gurnett, D.A., Brain, D.A., 2011. Areas of enhanced ionization in the deep nightside ionosphere of Mars. J. Geophys. Res. 116, E06006. http://dx.doi.org/10.1029/2011JE003804.

Němec, F., Morgan, D.D., Gurnett, D.A., Duru, F., Truhlík, V., 2011. Dayside ionosphere of Mars: Empirical model based on data from the MARSIS instrument. J. Geophys. Res. 116, E07003. http://dx.doi.org/10.1029/2010JE003789.

Nielsen, E. et al., 2006. Observations of vertical reflections from the topside martian ionosphere. Space Sci. Rev. 126, 373–388.

Nielsen, E. et al., 2007. Local plasma processes and enhanced electron densities in the lower ionosphere in magnetic cusp regions on Mars. Planet. Space Sci. 55, 2164–2172.

Pätzold, M., Tellmann, S., Häusler, B., Hinson, D., Schaa, R., Tyler, G.L., 2005. A sporadic third layer in the ionosphere of Mars. Science 310, 837–839.

Richards, P.C., Fennelly, J.A., Torr, D.G., 1994. EUVAC: A solar EUV flux model for aeronomic calculations. J. Geophys. Res. 99, 8981–8992.

Titheridge, J.E., 1997. Model results for the ionospheric E region: Solar and seasonal changes. Ann. Geophys. 15, 63–78.

Watanabe, K., Masuda, S., Segawa, T., 2012. Hinode flare catalogue. Solar Phys. 279, 317–322.

Withers, P., 2009. A review of observed variability in the dayside ionosphere of Mars. Adv. Space Res. 44, 277–307.

Withers, P., Mendillo, M., 2005. Response of peak electron densities in the martian ionosphere to day-to-day changes in solar flux due to solar rotation. Planet. Space Sci. 53, 1401–1418.

Withers, P., Mendillo, M., Rishbeth, H., Hinson, D.P., Arkani-Hamed, J., 2005. Ionospheric characteristics above martian crustal magnetic anomalies. Geophys. Res. Lett. 32, L16204. http://dx.doi.org/10.1029/2005GL023483.

Withers, P., Mendillo, M., Hinson, D.P., Cahoy, K., 2008. Physical characteristics and occurrence rates of meteoric plasma layers detected in the martian ionosphere by the Mars Global Surveyor Radio Science experiment. J. Geophys. Res. 113, A12314. http://dx.doi.org/10.1029/2008JA013636.

Zou, H., Wang, J.-S., Nielsen, E., 2006. Reevaluating the relationship between the martian ionospheric peak density and the solar radiation. J. Geophys. Res. 111, A07305. http://dx.doi.org/10.1029/2005JA011580.